Available online at www.sciencedirect.com
SCIENCE DIRECT®
Solid State Ionics 159 (2003) 223–232
SOLID STATE IONICS
www.elsevier.com/locate/ssi

Synthesis and electrochemical performance of tetravalent doped $LiCoO_2$ in lithium rechargeable cells

S. Gopukumar[a,*], Yonghyun Jeong[b], Kwang Bum Kim[b]

[a] Central Electrochemical Research Institute (CSIR), Karaikudi-630 006, India
[b] Division of Material Science and Engineering, Yonsei University, 134, Shinchon-dong, Seodaemun-gu, Seoul 120-749, South Korea

Received 29 August 2002; received in revised form 27 January 2003; accepted 6 February 2003

Abstract

Titanium-doped lithium cobalt oxides having the formula $LiTi_xCo_{1-x}O_2$ ($0 \le x \le 0.5$) have been synthesized using high temperature solid-state technique and its performance in a lithium rechargeable cell is reported. The synthesized oxides were structurally analyzed using X-ray diffraction (XRD) and Raman spectroscopy. It has been observed that single-phase materials were below 10% of Ti doping whereas impurity spinel phases were detected at higher concentrations. Electrochemical behaviors of the prepared powders were analyzed using cyclic voltammetry (CV) and galvanostatic charge/discharge cycling studies in the voltage range 3.0–4.25 V (vs. Li metal) using 1 M $LiClO_4$/PC as electrolyte. The composition with $x = 0.01$ exhibits an initial charge and discharge capacity of 157 and 148 mA h/g at 0.2*C* rate, respectively, as compared to 137 and 134 mA h/g of $LiCoO_2$. Further, more than 90% of the capacity is retained even after 10 cycles. The role of tetravalent doping on the electrochemical behavior of $LiCoO_2$ has not been reported previously.

Keywords: Lithium Intercalation; Doping; Electrochemical properties; $LiCoO_2$; Capacity

1. Introduction

Lithiated transition metal oxides, namely, $LiMn_2O_4$, $LiCoO_2$ and $LiNiO_2$, are primarily used as cathode materials in lithium ion cells [1–5]. Among these, $LiCoO_2$ is the preferred material in majority of the commercial cells in view of its ease of synthesis and high reversibility [6]. The use of $LiCoO_2$ is considered to deliver a theoretical capacity of 273.8 mA h/g, i.e., when whole of the lithium is deintercalated. Although this high capacity looks very attractive from battery point of view, practically, only 50% of the theoretical capacity, i.e., ~ 137 mA h/g, is possible due to structural degradation and thereby limiting the extraction of lithium to 0.5 [7]. Recently, attempts to modify the pristine $LiCoO_2$ by using techniques like coating [8,9], mixing of ceramic oxide [10], etc. have been made with the idea of enhancing the practical capacity output by stabilizing the layered structure. In spite of the fact that some of these modifications have led to good capacity retention, partial doping of $LiCoO_2$ seems to be most acceptable approach for commercial exploitation consider-

* Corresponding author. Tel.: +91-4565-227750; fax: +91-4565-227779.
E-mail address: deepika_41@rediffmail.com (S. Gopukumar).

0167-2738/03/$ - see front matter © 2003 Elsevier Science B.V. All rights reserved.
doi:10.1016/S0167-2738(03)00081-X

ing the economy and ease of the bulk production process involved.

Ohzuku et al. [11] suggested that partial doping of cobalt with metal ions leads to extended cyclability and increase in capacity of lithium ion cells by enhancing structural stability. Further, theoretical studies suggest [12] that the capacity of layered compounds increased with partial transition metal ion substitution while on the other hand operating voltage increased by doping with nontransition metal ion at the expense of capacity [13–15]. Considering these predictions and a survey of literature suggests that studies on the effect of doping cobalt in $LiCoO_2$ with either of the metal ions like nickel [16], manganese [17], chromium [18], aluminum [19], boron [20], rhodium [21] or iron [22] have been carried out for understanding the electrochemical behavior of $LiM_xCo_{1-x}O_2$ (M = metal ions) in lithium ion cells. Among these materials, aluminum [15,23,24] and nickel [16] have received wide attention but marginal success towards increasing the performance has been reported with only partial nickel substitution. Hence, as evident from literature, doping of $LiCoO_2$ with +2 and +3 valent metal ions does not enhance the capacity over pristine $LiCoO_2$ and therefore alternative dopant ions have to be investigated.

Recently, it was reported by Kim and Amine [25] that the capacity of layered $LiNiO_2$ could be enhanced by doping with tetravalent ions. As $LiNiO_2$ and $LiCoO_2$ are layered materials, therefore, we found it worthwhile to carry out a systematic investigation on the effect of a tetravalent ion by partially substituting cobalt in pristine $LiCoO_2$. We believe that the presence of tetravalent ions leads to the presence of some Co^{2+} charge compensators and, moreover, since both $LiCoO_2$ and $LiTiO_2$ [26] are isostructural, solid solution could be formed thereby enhancing the performance of the end members. A survey of literature points out only a sole publication [27] reporting the IR and Raman spectra of only $LiTi_{0.2}Co_{0.8}O_2$ synthesized at high and low temperatures. We were therefore interested to carry out a detailed investigation on the electrochemical behavior of $LiTi_xCo_{1-x}O_2$ ($x = 0.01-0.5$) as a cathode material for lithium rechargeable cells and present in this communication new electrochemical results hitherto not reported.

2. Experimental

High purity lithium hydroxide, cobalt acetate and titanium dioxide (Aldrich Chemical, USA) were used as received for the synthesis of $LiCoO_2$ and $LiTi_xCo_{1-x}O_2$ by solid-state technique. Stoichiometric amounts of the above chemicals with slight excess of lithium were weighed, mixed thoroughly and then heated initially at 400 °C for 6 h and then annealed at 800 °C for 12 h in a tubular furnace. The heating rate was controlled at 1 °C/min and then cooled at same rate to room temperature. The powders were ground well and used for physical and electrochemical investigations.

The structure of the synthesized powders were evaluated with an automated Rigaku powder X-ray diffractometer using Cu-K_α radiation by measuring the diffraction angle (2ϑ) between 10° and 80° with an increment of 0.02°/min. XRD of the cycled electrodes were also recorded for analyzing the structural changes.

Room temperature Raman spectra were recorded for the synthesized pristine $LiCoO_2$ as well as Ti-doped $LiCoO_2$ using Jobin-Yvon ISA T64000 Raman spectrometer equipped with a CCD detector and a microscope. Powder samples were put under a microscope objective that allows the laser beam to focus on a small selected area of the surface ($\sim 1\ \mu m^2$) and the backscattered Raman signal was collected. The laser light source was 514.5 nm line excited at 5–10 mW at an Ar ion laser power. A typical spectral run took only a few minutes, hence five Raman spectra, each recorded over the frequency 400–800 cm^{-1} at an acquisition time of 400 s, were averaged to increase the signal to noise ratio.

XANES measurements were recorded for the synthesized materials as detailed elsewhere [40].

Scanning electron microscope (SEM, Hitachi, S2700) was used for observing the morphology of the synthesized powders.

Electrodes for electrochemical measurements consisted of slurry prepared from a mixture of the synthesized powder with carbon black and PVDF binder in the ratio of 85:10:5, respectively, with NMP solvent. The slurry was coated onto an aluminum foil current collector and dried for 3 h. The electrode was hot pressed and stored in an argon-filled glove box prior to use. Cyclic voltammetry (CV) and

charge/discharge cycling studies were carried out using a three-electrode glass cell with 1 M $LiClO_4$/PC as electrolyte. Lithium foil was used both as reference and counter electrodes. CV experiments were performed at a scan rate of 25 μV/s in the potential range 3.5–4.25 V. Galvanostatic charge/discharge studies were carried out at a current rate of *C*/5 in the potential range 3–4.25 V. All electrochemical measurements were performed inside an argon-filled glove box and data recorded with an automated battery cycle life tester.

3. Results and discussion

$LiCoO_2$ has an α-$NaFeO_2$ structure belonging to *R*-3*m* space group, in which Li and Co ions are arranged alternatively occupying the 3b and 3a sites, respectively, and sandwiched between oxygen ions. Recently, it has been reported that spinel ($LiTi_2O_4$) [28] compounds of lithium and titanium could be synthesized and can be used in lithium batteries. However, these materials are found to be electrochemically active only in the voltage range below 3 V. In the present investigation, we see that the synthesized materials (below Ti doping of 10%) are capable of cycling at higher voltages, i.e., up to 4.25 V, and hence, no spinel phase lithium titanate is formed below $x=0.10$. Theoretical studies of Ceder et al. [14] suggest the formation of $LiTiO_2$ having the α-$NaFeO_2$ structure, but practically, it was observed by Obrovac et al. [26] that even though layered $LiTiO_2$ could be synthesized, deintercalation of lithium was not possible. Moreover, Pouillerie et al. [29] concluded from their study on $LiNi_{1-x}Mg_xO_2$ that for small values of x (below 10%), magnesium ions occupy the lithium sites due to larger ionic radii of magnesium (0.76 Å) than nickel. Following the above views, one may expect that partial introduction of Ti^{4+} ions in place of Co^{3+} in the present case could lead to the presence of titanium in lithium sites since the ionic radii of titanium ions (0.605 Å) are larger as compared to cobalt (0.545 Å) ions. This assumption can also be safely ruled out in view of the smaller ionic size of titanium as compared to lithium and also its high positive charge [30]. Therefore, we can say that addition of low amounts ($x<0.1$) of Ti corresponds to simple replacement of Co in the CoO_2 layers, Co^{2+} being the charge compensator, i.e., $[Li]_{3b}[Co_{1-x}Ti_x]_{3a}O_2$. Similar model has been postulated by Tukamoto and West [31] on their study on Mg-doped $LiCoO_2$. Further, very recent studies of Croguennec et al. [32] on the Rietveld analysis of Ti^{4+}-doped $LiNiO_2$ confirm the presence Ti^{4+} in the nickel site ($[Li_{1-z}Ni_z^{2+}]_{3b}[Ni_{t+z}^{2+}Ti_t^{4+}Ni_{1-z-2t}^{3+}]_{3a}O_2$). Moreover, the materials synthesized in the present study reveal that a layered structure of $LiTi_xCo_{1-x}O_2$ is applicable only up to a value of $x<0.1$ wherein the oxidation state is maintained around 3 [33]. Thus, we may say that true solid solutions of Li_2TiO_3 and $LiCoO_2$ are possible only at low concentration of titanium ions.

Having ascertained the formation of layered $LiTi_xCo_{1-x}O_2$ following the above discussions, we now make structural analysis using XRD and Raman spectroscopy for confirming our postulations. Fig. 1(i) presents the X-ray diffraction patterns of all the synthesized powders of $LiTi_xCo_{1-x}O_2$ in the composition range $0 \le x \le 0.5$. It is observed from the X-ray patterns that the entire fingerprint peaks, viz., 003, 101, 006, 102, 104, 108 and 110, are clearly identifiable thereby suggesting the formation of the α-$NaFeO_2$ structure. The diffraction peaks of the synthesized pristine $LiCoO_2$ are in excellent agreement with the JCPDS card No. 16-0427. The patterns also indicate the existence of additional impurity peaks from a composition of $LiTi_{0.05}Co_{0.95}O_2$ (Fig. 1(i)c) and increases in intensity with further increase in titanium composition. Further, at higher compositions of titanium, a shoulder peak emerges alongside the 003 peak and the intensity of doublet peaks (006, 102, 108 and 110) also diminishes. Therefore, we can confirm from the present solid-state synthesis that true solid solutions of the type $LiTi_xCo_{1-x}O_2$ is possible only below the composition of $x=0.05$. The hexagonal parameters of the synthesized materials are presented in Table 1. As is well known, the lattice parameter a represents the intralayer metal–metal distance while c is ascribed to inter slab distances. It can be seen from Table 1 that the a and c values for synthesized pristine $LiCoO_2$ are 2.816 and 14.05 Å, respectively. These values are in excellent agreement with the reported values of FM, USA [34] and other researchers [16,23]. Furthermore, c/a ratio is an indicator of the metal–metal layering distance or in other words hexagonal setting, and is

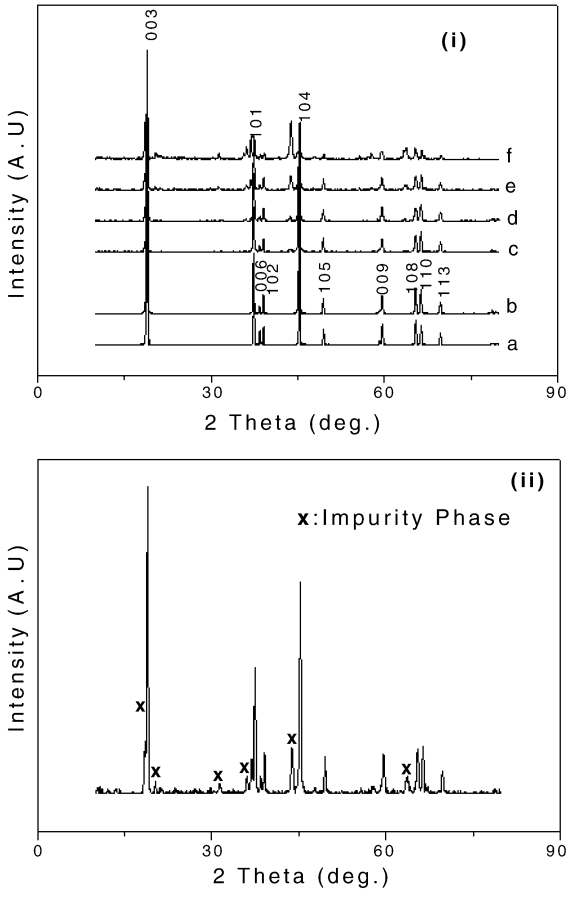

Fig. 1. (i) XRD pattern of $LiTi_xCo_{1-x}O_2$ (a: $x=0$; b: $x=0.01$; c: $x=0.05$; d: $x=0.10$; e: $x=0.25$; f: $x=0.50$). (ii) XRD pattern of $LiTi_{0.25}Co_{0.75}O_2$.

also found to be in close agreement with the reported values, i.e., 4.989.

We have not carried out Rietveld analysis, but to a very good approximation, the intensities of the XRD fingerprint peaks and Raman spectra studies can predict cation mixing. It can be noted that the ratio of the intensities of 003 and 104 (I_{003}/I_{104}) peaks is greater than unity, thereby suggesting no cation disorder which is supplemented by the values of c/a, i.e., >4.89. Interestingly, it is seen that the ratio of the intensities of 003 and 104 peaks for pristine $LiCoO_2$ is around 2.67 and is the highest [21]. Further, as can be seen from Table 1, the c/a ratios are in the range of 4.98 thereby indicating no cation mixing. However, coexistence of other impurities with the layered structure is seen by the presence of many additional peaks at higher titanium compositions ($>x=0.10$) and can be ascribed due to inhomogeneous distribution of Ti ions in the $LiCoO_2$ oxide matrix.

Looking at the radius of Ti^{4+} (0.605 Å) [30], we can expect that the partial replacement for low spin Co^{3+} (0.545 Å) should increase the a and c values thereby facilitating easy lithium insertion and extraction. We observe similar trend up to a value of $x=0.05$ beyond which the values decreases. This could be due to the growth of additional impurity phases at higher titanium concentrations leading to decreased electrochemical activity. Following the suggestions of Reimers et al. [35], we observe that the R factor, i.e., the ratio of $[I_{006}/I_{102}]/I_{101}$, is minimum for the lowest dopant composition, viz., $LiTi_{0.01}Co_{0.99}O_2$, and therefore suggesting increased layered characteristics than the pristine $LiCoO_2$ and other titanium compositions. These factors along with the well-defined splitting of doublet peaks at 108 and 110 coupled with high value of lattice constants a, c as well as c/a ratio indicate that this composition should have improved electrochemical performance.

The synthesized pristine and Ti-doped $LiCoO_2$ materials has a layered structure and can be assigned to the space group R-3m and the atoms (Co, Li and O) are located in the Wychoff sites 3a, 3b and 6c, respectively. Factor group analysis [36] of the Raman Spectra for pristine $LiCoO_2$ suggests a pair of intense peaks located around frequencies of 595 and 485 cm^{-1} and is ascribed to Raman active modes A_{1g} and E_g, respectively. Since Raman modes are entirely due to oxygen atoms, hence the symmetry motions involve Co–O stretching and O–Co–O bending vibrations. The peak at frequency 595 cm^{-1} can be ascribed to symmetric Co–O stretching vibrations of cobalt octohedra [37]. Inaba et al. [38] observed the broadening of the peaks with increasing values of x on

Table 1
XRD lattice parameters a and c (Å) and intensity ratios of 003 and 104 peaks (I) for $LiTi_xCo_{1-x}O_2$

x	a	c	c/a	I
0	2.8163	14.051	4.989	2.67
0.01	2.8170	14.072	4.995	1.45
0.05	2.8168	14.070	4.995	1.23
0.25	2.8148	14.068	4.998	–
0.50	2.8121	14.029	4.989	–

their study on $LiNi_xCo_{1-x}O_2$. However, broadening of these peaks was ascribed due to polyhedral distortion in pristine $LiCoO_2$ [37]. Based on the intensities of the peaks (Fig. 2a) for pristine $LiCoO_2$, the peaks located at 485.4 and 594.6 cm^{-1} correspond to the optical modes Eg and A_{1g}, respectively, and are as predicted. Thus, A_{1g} stretching mode must be at a higher frequency than the Eg bending mode. Further, with increasing titanium doping, the peaks become broader as predicted by Inaba et al. [38]. It can be clearly seen that the synthesized pristine $LiCoO_2$ has no impurity peaks. However, as seen from Fig. 2b and c, the intensities of the peaks decrease and become broader at lower titanium doping contents, indicating the incorporation of Ti into Co sites. However, at higher doping levels (Fig. 2c), we observe the appearance of additional peaks located at frequencies of 447.8, 604.4 and 686.1 cm^{-1}. Thus, it is clearly seen that a spinel phase coexists with the layered structure and is consistent with our XRD spectrum, wherein we observe a peak growing alongside the 003 peak as also other additional peaks [marked × in Fig. 1(ii)]. Furthermore, due to lack of excess lithium required for the formation of both the phases, Co_3O_4 impurities are also traceable by the appearance of broad Raman peak located at a frequency of 686.1 cm^{-1}. Therefore, we can say that single-phase layered structure is observed only at lower titanium doping levels whereas spinel and impurity phases coexist at higher dopant levels.

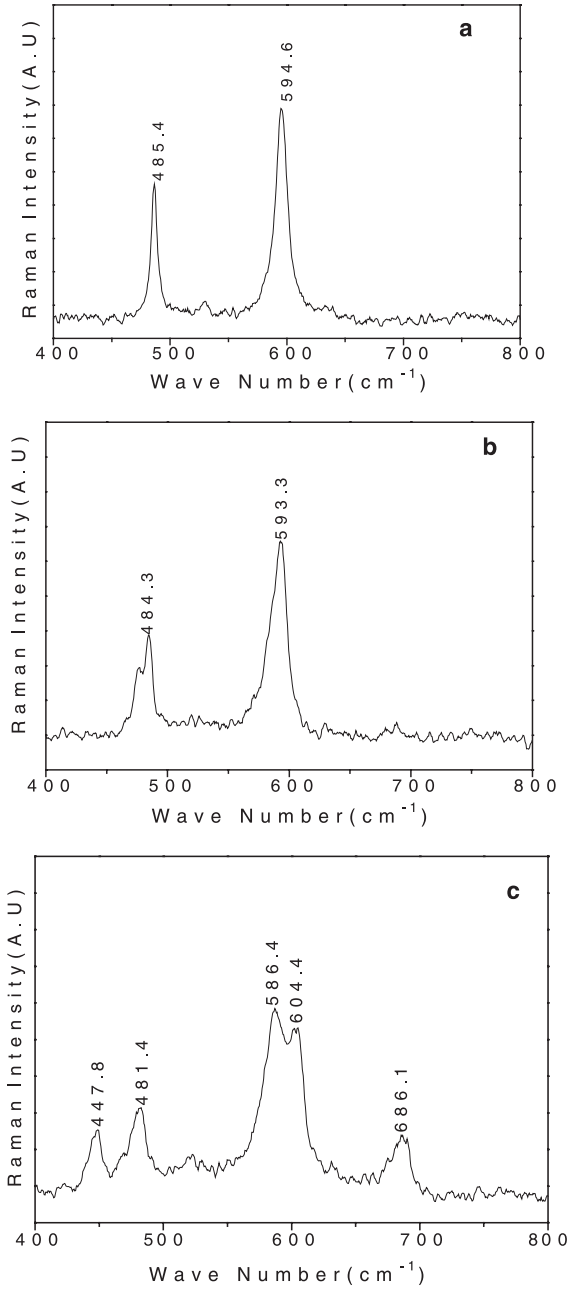

Fig. 2. Raman spectra of $LiTi_xCo_{1-x}O_2$ (a: $x=0$; b: $x=0.01$; c: $x=0.25$).

The synthesized materials were analyzed using XANES spectroscopy technique for obtaining meaningful information on the oxidation state of the metal in the bulk state. Fig. 3a presents the Co K-edge XANES spectra for the synthesized pristine and Ti-doped $LiCoO_2$. It can be clearly seen that the pattern of the spectra for the pristine $LiCoO_2$ is similar to literature reports [40]. The characteristic pre-edge peak 'A', region 'B' and a strong absorption peak 'C' assigned to the dipole-forbidden 1s to 3d, 1s to 4p as well as to the metal ligand transfer- and dipole-allowed 1s to 4p, respectively, are clearly noticeable. Furthermore, it is interesting to note from region 'B' (an indicator of the oxidation state of the metal ion) that the presence of minor amounts of titanium doping shifts the edge energy to slightly lower position thereby suggesting the presence of some Co^{2+} (Fig. 3b-ii) by the incorporation of Ti^{4+}. However, on the other hand, the edge energies shift to higher values with the increase in Ti^{4+} contents indicating the presence of Co^{4+} (Fig. 3b-iii) ions due to the inhomogeneous mixing of Ti ions in the $LiCoO_2$ oxide

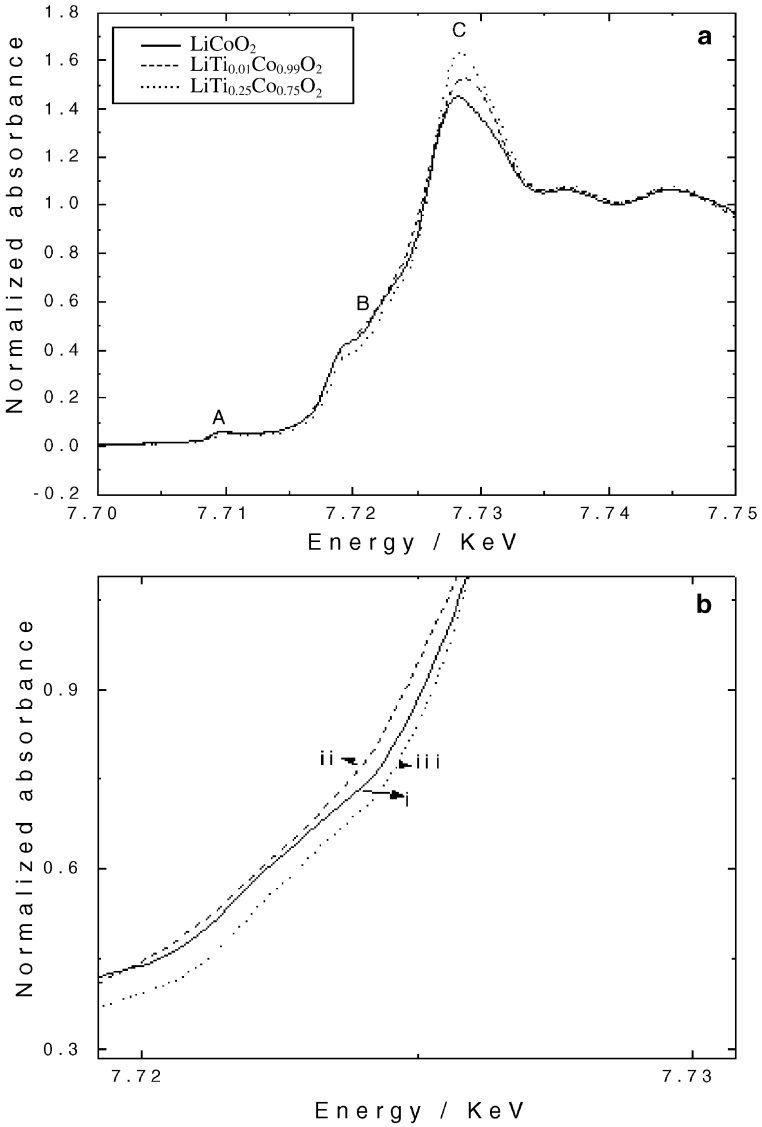

Fig. 3. (a) XANES spectra of $LiTi_xCo_{1-x}O_2$. (b) Magnified view of region B of XANES spectra of $LiTi_xCo_{1-x}O_2$ (i: $x=0$; ii: $x=0.01$; iii: $x=0.25$).

matrix. Detailed discussions on the spectral aspects of the synthesized materials will be presented in a subsequent publication in accordance with Ref. [44].

Morphology of the titanium-doped $LiCoO_2$ depicts that the particles are polydispersed with an average size of less than 1 μm. A typical SEM photograph is presented in Fig. 4.

Cyclic voltammetry is a useful electrochemical tool wherein the changes taking place in an electrochemical reaction are monitored by measuring the current–potential responses. Typical CVs obtained in the present case are depicted in Fig. 5. It is clear from the figures that the major oxidation and reduction peaks are observed at around 3.95 and 3.75 V, respectively, and are representative of lithium deintercalation and reintercalation processes, respectively. These peaks are also signature of hexagonal phase in these types of layered compounds and indicating

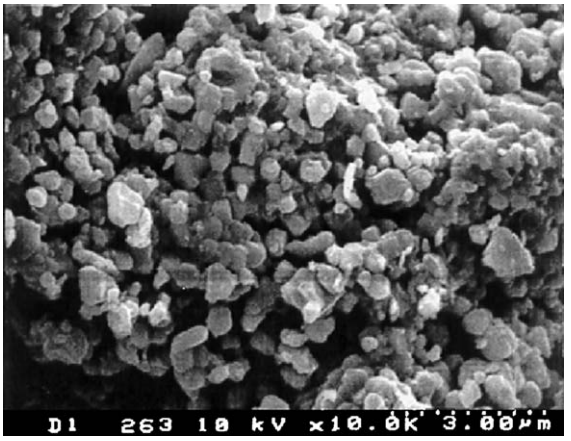

Fig. 4. A typical SEM of $LiTi_{0.01}Co_{0.99}O_2$.

perfect reversibility. Further, two very low intensity small high voltage peaks are also noticed both in the oxidation as well as in the reduction process at around 4.08 and 4.17 V depicting the coexistence of monoclinic phases in the investigated materials. It should be emphasized here that these high voltage peaks in pristine $LiCoO_2$ in the present case are detectable but grow with increase in titanium doping. The high voltage peaks are slightly better visible in the $x=0.01$ concentration and become very prominent at $x=0.25$ (Fig. 5c). This assumption is supported by the fact that in the case of $LiCoO_2$, the high voltage peaks are very prominent with decrease in particle size as observed by Uchida and Saito [39] on their study of thin films and also in the case of sol–gel [40] synthesized $LiCoO_2$. Our results of CV of $LiCoO_2$ are in agreement with Reimers and Dahn [41]. Further, the high voltage peaks are a debatable issue [42] as some of the workers have not observed such peaks. Moreover, these two peaks are assigned due to the phase transition between ordered and disordered lithium ion arrangement in the CoO_2 sheets. It was suggested by Yazami et al. [43] that these high voltage peaks could also arise out of anion absorption on surface impurities. In the present case, we see that these peaks are growing (Fig. 5c) with increasing titanium content (0.25) and therefore we may ascribe this is due to the inhomogeneous distribution of Ti in the $LiCoO_2$ oxide matrix. Similar behavior in CV studies was observed in the case of rhodium-doped $LiCoO_2$ [21]. Furthermore, as these peaks occur at exactly the same voltage as that of monoclinic phase, therefore, the ordering/disordering of Ti–Co ions also takes place reversible to Li ions in this phase. This can be confirmed with the growth of additional peaks in the XRD spectrum more so with the splitting of 104 peak initiating from $x=0.1$ composition.

Fig. 6 depicts the capacities of the synthesized pristine $LiCoO_2$ and titanium-doped $LiCoO_2$ materials over the entire composition range investigated for 10 cycles. It can seen that the composition with $x=0$, i.e., $LiCoO_2$ delivers the charge and discharge capacities of 137 and 134 mA h/g, respectively, for the first cycle at a current rate of $C/5$ in the voltage range of 3–4.25 V. The very low irreversible capacity of 3 mA

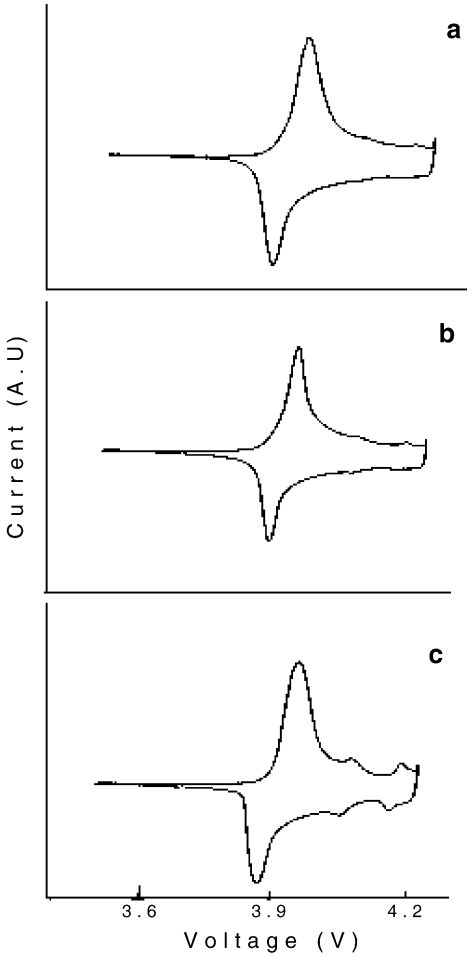

Fig. 5. Cyclic voltammograms of $LiTi_xCo_{1-x}O_2$ (a: $x=0$; b: $x=0.01$; c: $x=0.25$).

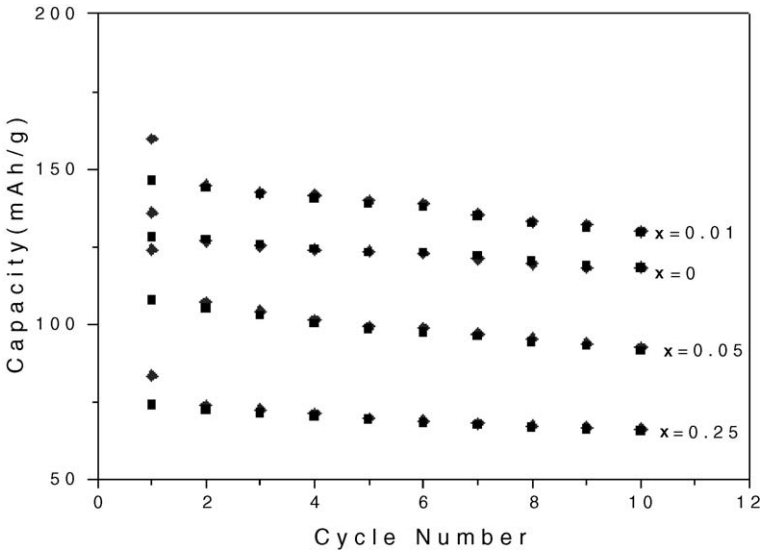

Fig. 6. Capacity (mA h/g) dependence on cycle number for $LiTi_xCo_{1-x}O_2$.

h/g confirms the purity of our sample and from second cycle onwards there is hardly any difference in the charge and discharge capacities. Moreover, we find that about 96% (128 mA h/g) of the initial capacity is retained after 10 cycles and corresponds to ~ 0.5 of lithium extraction during the charging process. The loss of capacity (3 mA h/g) in the first cycle can be assigned to the formation stage. The obtained values of capacity for pristine $LiCoO_2$ are the highest achieved and compare well with the literature reports [7]. Analysis of the doped $LiCoO_2$ samples indicates that the sample with $x=0.01$ delivers the highest capacity. The fist charge and discharge capacities of $LiTi_{0.01}Co_{0.99}O_2$ are 157 and 148 mA h/g, respectively. This implies a loss of 9 mA h/g in the first cycle as compared to 3 mA h/g for $LiCoO_2$. This slight higher initial loss is understandable in view of the presence of the inactive Ti^{4+} species present in the Co sites. Even though the initial capacity loss is more in the case of $x=0.01$, in subsequent cycles, the loss is not noticed similar to $LiCoO_2$ and the capacities are retained at 135 mA h/g after 10 cycles (Fig. 7). This result is interesting in view of the fact that we have obtained higher capacities than pristine $LiCoO_2$. We confirmed the composition of this particular sample using ICP-AES in view of its superior performance and note that, as expected, the compositions of Ti and Co were 0.009 and 0.991, respectively. Thus, we can confirm the positive effect of tetravalent substitution to the layered structure. Furthermore, as observed in XRD patterns, the well-defined doublets at 006, 102 as well as at 108 and 110 coupled with an increase in the lattice parameters a and c endorse the high electrochemical performance of this investigated composition. Having encouraged by this composition, we investigated other higher compositions and found that the capacities gradually decreased with further increase in titanium content thereby indicating that this composition is the optimum level of dopant. One interesting point to note here is that the presence of higher content of titanium improves the cyclability but

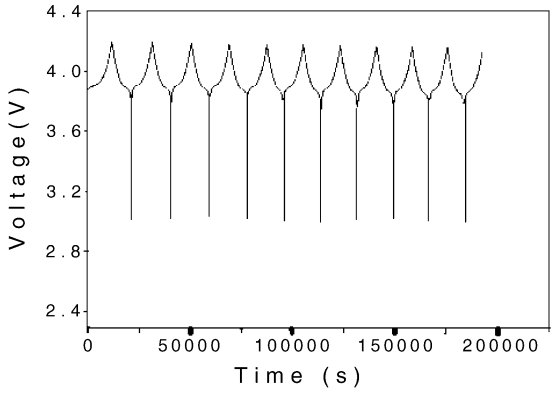

Fig. 7. Cycling behavior of $LiTi_{0.01}Co_{0.99}O_2$.

at the expense of capacity, which is understandable due to the reduction in cobalt ions and as reiterated earlier the electrochemically inactive nature of titanium ions in the investigated voltage range. As observed in the XRD patterns of the cycled $LiTi_{0.01}Co_{1-x}O_2$ cathode (Fig. 8), the structure of the synthesized material is retained even after 10 cycles thereby suggesting the stability of the material. Further, spectral and rate capability studies on this material correlating the present observations have recently been reported elsewhere [44].

Literature survey indicates that various dopants like Ni, Mg, Mn, Zn, Rh, Al, B, Fe, etc. [15,17,21,22,45] substituted for cobalt in $LiCoO_2$ have demonstrated inferior capacities than reported in this study for $LiTi_{0.01}Co_{0.99}O_2$ (Fig. 6) in the voltage range 3–4.25 V.

During the preparation of this manuscript, we came across a recent report by Choblet et al. [10] wherein the authors claim high capacities by the addition of minor amounts of TiO_2 (2 wt.%) as a distinct second phase to $LiCoO_2$ synthesized by complex sol–gel process. Indeed, our results also indicate an enhancement in capacity over pristine $LiCoO_2$ but have several advantages than the former like elimination of chelating agent (ascorbic Acid), pH maintenance (NH_4OH), lower titanium content (1%) and, above all, simple synthesis procedure. Further, our results can be supported by recent findings of Kim and Amine [25] on the role of tetravalent substitution in $LiTi_xNi_{1-x}O_2$ system. The authors also found that a composition of $x=0.025$ gave a enhanced capacity in the voltage range 2.8–4.3 V. The amount of titanium needed to stabilize the $LiNiO_2$ structure is slightly higher than in the present case. Of course, this is understandable in view of the fact that complete oxidation of nickel ions is difficult due to their presence in lithium layers. Therefore, we may conclude that the substitution of low amounts of titanium for cobalt in $LiCoO_2$ results in enhanced electrochemical performance.

4. Conclusion

We have demonstrated that it is possible to prepare solid solutions of $LiCoO_2$ and Li_2TiO_3 using high temperature solid-state technique. Structural characterization using XRD and Raman spectra reveals that single-phase layered compounds with α-$NaFeO_2$ structure are attained at lower titanium doping. The rate of capacity looks similar irrespective of doping amount, even though the initial capacity was enhanced a little for the case of low-doped sample. Further, enhanced stable electrochemical capacities of 135 mA h/g at a current rate of $C/5$ have been achieved for the composition $LiTi_{0.01}Co_{0.99}O_2$ in a lithium rechargeable cell in the voltage range 3–4.25 V using $LiClO_4$/PC as electrolyte.

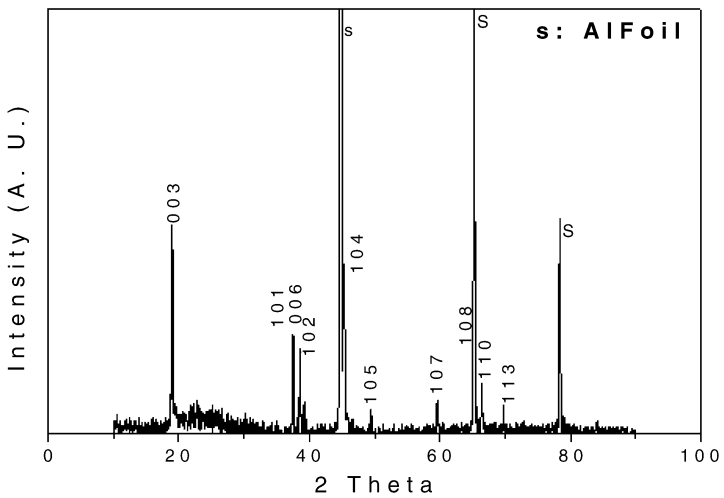

Fig. 8. XRD pattern of cycled $LiTi_{0.01}Co_{0.99}O_2$.

Acknowledgements

One of the authors, GK, would like to thank KOFST, Seoul, Korea, for offering a Brain Pool Visiting Fellowship. GK also thanks CECRI, Karaikudi and CSIR, New Delhi, for grant of leave. The authors thank the referees for their valuable suggestions. This work was also supported by the Ministry of Information and Communication of Korea (Support Project of University Information Technology Research Center supervised by KIPA). The authors would like to thank Cheil Industries Inc. for supporting electrolyte.

References

[1] T. Nagaura, K. Tozawa, Prog. Batteries Sol. Cells 9 (1990) 209.
[2] B. Scrosati, Nature 373 (1993) 557.
[3] L.B. Lave, C.T. Henrickson, F.C. McMicheal, Science 268 (1993) 993.
[4] M. Broussely, P. Bieusan, B. Simon, Electrochim. Acta 45 (1999) 3.
[5] C. Delmas, in: G. Pistoia (Ed.), Lithium Batteries—A New Materials Developments and Perspectives, Elsevier, Amsterdam, 1994, pp. 457–489, Chap. 12.
[6] C. Julien, S. Gastro-Garcia, J. Power Sources 97/98 (2001) 290.
[7] Z. Lu, D.D. MacNeil, J.R. Dahn, Electrochem. Solid-State Lett. 4 (2001) A200.
[8] J. Cho, J.Y. Kim, B. Park, Chem. Mater. 12 (2000) 3788.
[9] J. Cho, J.Y. Kim, B. Park, J. Electrochem. Soc. 148 (2001) A1110.
[10] A. Choblet, H.C. Shia, H.-P. Liu, M. Salomon, A. Mannivannan, Electrochem. Solid-State Lett. 4 (2001) A65.
[11] T. Ohzuku, A. Udea, M. Nagayama, Y. Iwakoshi, H. Konnori, Electrochim. Acta 38 (1993) 1159.
[12] S. Venkatraman, V. Subramanian, S. Gopukumar, N.G. Renganathan, N. Muniyandi, Electrochem. Commun. 2 (2000) 18.
[13] G. Ceder, Y.M. Chiang, D.R. Sadoway, M.K. Aydinol, Y.I. Jang, B. Huang, Nature 392 (1998) 894.
[14] G. Ceder, M.K. Aydinol, A.F. Kohan, Comput. Mater. Sci. 8 (1997) 161.
[15] W. Yoon, K.K. Lee, K.B. Kim, J. Electrochem. Soc. 147 (2000) 2023.
[16] I. Sadoune, C. Delmas, J. Solid State Chem. 136 (1998) 8.
[17] C. Julien, M.A. Camacho-Lopez, T. Mohan, S. Chitra, P. Kalyani, S. Gopukumar, Solid State Ionics 135 (2000) 241.
[18] C.D.W. Jones, E. Rosen, J.R. Dahn, Solid State Ionics 68 (1994) 65.
[19] G.A. Nazri, A. Rougier, K.F. Kia, Mater. Res. Symp. Proc. 453 (1997) 63.
[20] R. Alcantara, P. Lavela, J.L. Tivado, R. Stoyanova, E.J. Zhecheva, Solid State Chem. 134 (1997) 265.
[21] S. Madhavi, G.V. Subba Rao, B.V.R. Chowdari, S.F.Y. Li, J. Electrochem. Soc. 148 (2001) A1279.
[22] H. Kobayashi, S. Shigemura, M. Tabuchi, H. Sakaebe, K. Ado, H. Kageyama, A. Hirano, R. Kanno, M. Wakita, S. Morimotoand Nasu, J. Electrochem. Soc. 147 (2000) 960.
[23] Y.I. Jang, B. Huang, H. Wang, D.R. Sadoway, G. Ceder, Y.M. Chiang, H. Liu, H. Tamura, J. Electrochem. Soc. 146 (1999) 862.
[24] H. Huang, G.V. Subba Rao, B.V.R. Chowdari, J. Power Sources 690 (1999) 81.
[25] J. Kim, K. Amine, Electrochem. Commun. 3 (2001) 52.
[26] M.N. Obrovac, O. Mao, J.R. Dahn, Solid State Ionics 112 (1998) 9.
[27] W. Huang, R. Frech, Solid State Ionics 86–88 (1996) 395.
[28] P. Krtil, D. Fattakhova, J. Electrochem. Soc. 148 (2001) A1045.
[29] C. Pouillerie, L. Croguennec, Ph. Biensan, P. Willmann, C. Delmas, J. Electrochem. Soc. 147 (2000) 2061.
[30] B.V.R. Chowdari, G.V. Subba Rao, S.Y. Chow, Solid State Ionics 140 (2001) 55.
[31] H. Tukamoto, A.R. West, J. Electrochem. Soc. 144 (1997) 3164.
[32] L. Croguennec, E. Suard, P. Willmann, C. Delmas, Chem. Mater. 14 (2002) 2149.
[33] Z. Lu, D.D. MacNeil, J.R. Dahn, Electrochem. Solid-State Lett. 4 (2001) A200.
[34] X.Q. Yang, X. Sun, J. McBreen, Electrochem. Commun. 2 (2000) 100.
[35] J.N. Reimers, E. Rossen, C.D. Jones, J.R. Dahn, Solid State Ionics 61 (1993) 335.
[36] W.G. Fateley, Infrared and Raman Selection Rules for Molecular and Lattice Vibrations: The Correlation Method, Wiley-Interscience, New York, 1972.
[37] C. Julien, M.A. Camacho-Lopez, L. Escobar-Alarcon, E. Haro-Poniatowski, Mater. Chem. Phys. 68 (2001) 210.
[38] M. Inaba, Y. Todzuka, H. Yoshida, Y. Grincourt, A. Tasaka, Y. Tomida, Z. Ogumi, Chem. Lett., (1995) 889.
[39] I. Uchida, H. Saito, J. Electrochem. Soc. 142 (1995) L139.
[40] W.S. Yoon, K.B. Kim, J. Power Sources 81–82 (1999) 517.
[41] J.N. Reimers, J.R. Dahn, J. Electrochem. Soc. 139 (1992) 2091.
[42] T. Ohzuku, A. Ueda, J. Electrochem. Soc. 141 (1994) 2972.
[43] R. Yazami, N. Lebrun, M. Bonneau, M. Molteni, J. Power Sources 54 (1995) 389.
[44] G. Kumar, K.W. Nam, H.S. Jung, K.B. Kim, 11th IMLB, Electrochemical Society Inc., California, 2002, p. 96.
[45] C. Julien, G.A. Nazri, A. Rougier, Solid State Ionics 135 (2000) 121.